NAVAL SHIP RESEARCH AND DEVELOPMENT CENTER
Washington, D.C. 20007

MEASUREMENT OF FORCES AND SPINDLE MOMENTS ON INDIVIDUAL BLADES OF A LARGE-HUBBED PROPELLER

by
Stephen B. Denny

DEPARTMENT OF HYDROMECHANICS
RESEARCH AND DEVELOPMENT REPORT

December 1969 Report 3252

MEASUREMENT OF FORCES AND SPINDLE MOMENTS ON INDIVIDUAL BLADES OF A LARGE-HUBBED PROPELLER Report 3252

The Naval Ship Research and Development Center is a U.S. Navy center for laboratory effort directed at achieving improved sea and air vehicles. It was formed in March 1967 by merging the David Taylor Model Basin at Carderock, Maryland and the Marine Engineering Laboratory at Annapolis, Maryland. The Mine Defense Laboratory, Panama City, Florida became part of the Center in November 1967.

Naval Ship Research and Development Center
Washington, D.C. 20007

NDW-NSRDC 3960/43 (10-6

DEPARTMENT OF THE NAVY

NAVAL SHIP RESEARCH AND DEVELOPMENT CENTER

WASHINGTON, D. C. 20007

MEASUREMENT OF FORCES AND SPINDLE MOMENTS ON INDIVIDUAL BLADES OF A LARGE-HUBBED PROPELLER

by

Stephen B. Denny

December 1969

Report 3252

TABLE OF CONTENTS

LIST OF FIGURES

LIST OF TABLES

NOTATION

c	Section chord length
D	Propeller diameter
d	Propeller hub diameter
F_s	Propeller side force
f_M	Blade section camber
J	Nondimensional advance coefficient $J = U/nD$
K_{F_s}	Side-force coefficient $K_{F_s} = F_s/\rho n^2 D^4$
K_M	Blade spindle-torque coefficient $K_M = M/\rho n^2 D^5$
K_Q	Propeller-torque coefficient $K_Q = Q/\rho n^2 D^5$
K_{Q_1}	Torque coefficient, single blade
K_{Q_6}	Torque coefficient, six blades
K_T	Propeller-thrust coefficient $K_T = T/\rho n^2 D^4$
K_{T_1}	Thrust coefficient, single blade
K_{T_6}	Thrust coefficient, six blades
L	Hull length
M	Blade-spindle torque
n	Propeller revolutions/time
P	Blade-section-pitch
Q	Propeller torque
R	Propeller radius
R_h	Hub radius
R_n	Reynolds number
r	Radial coordinate from propeller axis
r_m	Radial coordinate from propeller axis to blade midspan
S	Blade span
s	Blade spanwise coordinate
T	Propeller thrust
t	Blade-section maximum thickness
U	Vehicle speed

X	Axial hull coordinate measured from bow
x	Axial station of hull $x = X/L$
Y	Transverse hull coordinate, measured from axis
y	Nondimensional transverse hull coordinate $y = Y/2Y_{max}$
α	Blade effective angle of attack
δ	Differential blade pitch from design pitch
η_o	Propeller efficiency
ν	Kinematic viscosity of water
ρ	Density of water
ϕ	Blade pitch
$\phi(r)$	Local blade-section pitch

ABSTRACT

Axial forces, torque forces, and spindle moments were measured on the individual blades of a six-bladed large-hubbed propeller ($d/D \simeq 0.5$). Two different propeller-blade configurations were tested, and the hydrodynamic characteristics of each were determined over wide ranges of blade pitch and advance conditions. The experimental results indicated the peak forces and moments on propeller blades during emergency operating conditions as well as blade loads and propeller efficiencies during normal cruise operation. Also, by assuming a given blade rake relative to the propeller rotation plane and by vector resolution of the blade forces determined at zero advance for various pitches, it was possible to calculate the extent of propeller side-force capability during cyclic pitch operation.

The test results show that a mission requirement for large-hubbed cyclic-pitch propellers which calls for sizeable side-force capability for maneuvering will dictate the use of large blades that are not efficient in vehicle cruise modes. Recommendations are made for further investigations of blade-configuration and blade-rake effects on both propeller side-force capability and ahead propulsion.

ADMINISTRATIVE INFORMATION

This work was funded under Subproject SS-4636-0000, Task 12320, Problem 526-209.

INTRODUCTION

Large-hubbed propellers with raked blades and with independent cyclic and collective blade-pitch-changing capability have been proposed for application to submersible vehicles that require minimal speeds and high maneuverability.

The concept is simple; controlled changing of blade pitch enables a propeller to develop a wide variety of thrust values while maintaining rpm within a limited and more efficient range. Cyclic blade-pitch control produces varying values of blade axial force (thrust) and torque force at each circumferential position, and the summation of the forces for a propeller is a vector having components along and normal to the propeller axis. Blade rake alters orientation of the blade-lift vector, thereby contributing significantly to propeller side-force capability during

cyclic-pitch operation. Two such propellers in contrarotation at the bow and stern of a submersible vehicle offers the advantage of moment control about the longitudinal axis and any transverse axis; their use leads to six degrees of freedom of motion control for the vehicle.

Since the invention of large-hubbed propellers with individual blade control by Haselton,[1] considerable work has been done in the areas of machinery design, reliability, and performance prediction. Some experimental work has been conducted to determine propeller side-force capability but none has been carried out to measure individual blade-spindle torque, and little is known regarding ahead propulsive performance. In general, the blades considered were uncambered, without twist, and with a rectangular planform; a recent study by Hydronautics, Inc.[2] indicated that propeller systems utilizing these simple blade shapes were highly inefficient in cruise modes. No attempts had been made to develop a more efficient blade shape.

From the standpoint of powering and machinery design, it is necessary to have reliable data available on the hydrodynamic forces, moments, and spindle torque that act on the individual propeller blades of large-hubbed propellers during various phases of operation. For these reasons, a study was initiated at this Center with the following objectives:

1. To determine experimentally the hydrodynamic characteristics of untwisted, rectangular planform blades.

2. To test an alternate blade shape designed for increased efficiency in ahead operational modes.

3. To obtain sufficient hydrodynamic data on both blade configurations to enable estimates to be made of propeller efficiencies, side-force capabilities, and peak blade forces and spindle torques at emergency operating conditions.

---

[1]References are listed on page 29.

DESIGN AND DESCRIPTION OF TEST APPARATUS

The evaluation of powering and performance characteristics, including interaction effects, for a submersible vehicle having a propeller with a large hub would require using an integral hull and a propeller-model configuration that would be geometrically similar to a probable operational vehicle. However, since the quantities to be measured were limited to forces and spindle moments on the individual propeller blades, the major requirement was to satisfactorily represent the flow field into the blades rather than any particular hull-propeller configuration.

The TMB Model 5083 hull (formerly TMB Model 4198) was used for the tests. This well-streamlined body of revolution Series 58 form is 15 feet long and has a 10:1 fineness ratio. Figures 1a and 1b show the hull and model-propeller assembly; geometric offsets are listed in Table 1. The model was constructed principally of wood and had been modified to support an internal electric drive system. The drive unit was a stationary armature-rotating field system on which a hub assembly was mounted at an axial location 25 percent of the hull length from the bow. The hull slope at this point was only 3.0 degrees relative to the hull axis and, for all practical purposes, the inflow could be considered normal to nonraked, hub-mounted blades.

Figure 1b shows a closeup view of the propeller-hub assembly. The hub was 4 inches long, contoured to the hull, and constructed of six segments (three 30-degree arcs and three 90-degree arcs). A blade could be affixed on each hub segment and set by hand at a variety of angles. Each 90-degree hub segment was mounted firmly on the rotating field casing of the motor, and each was adjacent to 30-degree segments. The smaller segments were mounted on strain-gaged flexures that were attached to the rotating casing. The entire hub assembly rotated free from contact with the hull and consequently was flooded during submergence. The electric drive system was constructed with carbon-impregnated seals and was fed pressurized nitrogen during submergence to prevent flooding. The motor housing also contained sliprings through which input and output currents were transmitted to and from the strain-gaged flexures.

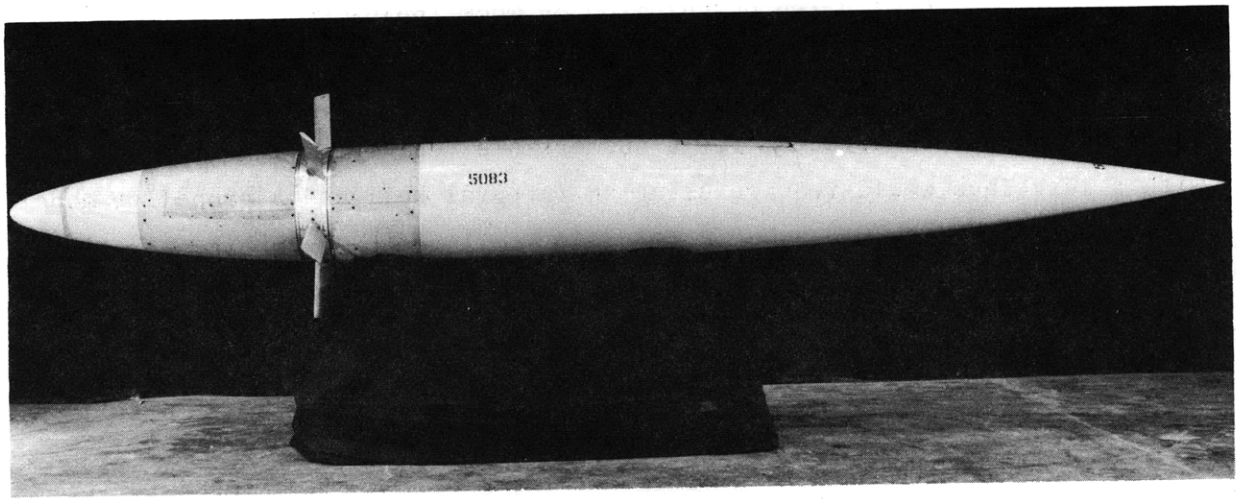

Figure 1a - Profile View of Hull

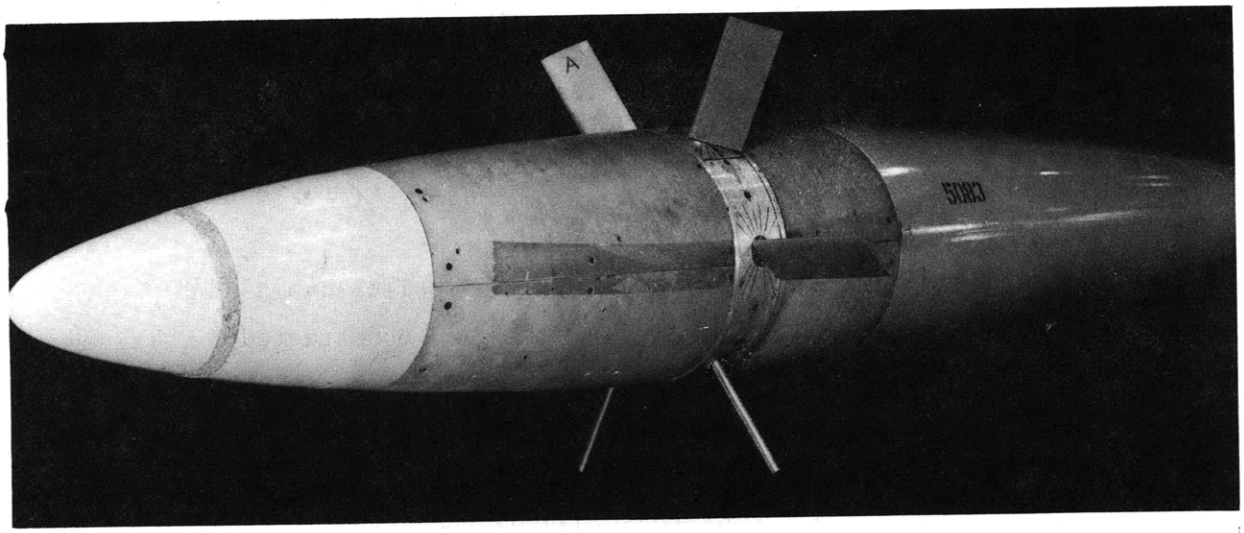

Figure 1b - Close View of Propeller-Hub Assembly

Figure 1 - Hull Model 5083 with Propeller Assembly

TABLE 1

Geometric Offsets of Hull Model 5083

x	X in.	y	Y in.	x	X in.	y	Y in.
0.00	000.0	0.0000	0.000	0.52	93.6	0.4818	8.672
0.02	3.6	0.1427	2.569	0.54	97.2	0.4755	8.559
0.04	7.2	0.2029	3.652	0.56	100.8	0.4684	8.431
0.06	10.8	0.2490	4.482	0.58	104.4	0.4603	8.285
0.08	14.4	0.2873	5.171	0.60	108.0	0.4513	8.123
0.10	18.0	0.3200	5.760	0.62	111.6	0.4414	7.945
0.12	21.6	0.3485	6.273	0.64	115.2	0.4305	7.749
0.14	25.2	0.3734	6.721	0.66	118.8	0.4187	7.537
0.16	28.8	0.3953	7.115	0.68	122.4	0.4058	7.304
0.18	32.4	0.4145	7.461	0.70	126.0	0.3919	7.054
0.20	36.0	0.4312	7.762	0.72	129.6	0.3768	6.782
0.22	39.6	0.4457	8.023	0.74	133.2	0.3605	6.489
0.24	43.2	0.4581	8.246	0.76	136.8	0.3429	6.172
0.26	46.8	0.4687	8.437	0.78	140.4	0.3239	5.830
0.28	50.4	0.4775	8.595	0.80	144.0	0.3036	5.465
0.30	54.0	0.4848	8.726	0.82	147.6	0.2817	5.071
0.32	57.6	0.4905	8.829	0.84	151.2	0.2582	4.648
0.34	61.2	0.4947	8.905	0.86	154.8	0.2330	4.194
0.36	64.8	0.4977	8.959	0.88	158.4	0.2060	3.708
0.38	68.4	0.4994	8.989	0.90	162.0	0.1771	3.188
0.40	72.0	0.5000	9.000	0.92	165.6	0.1461	2.630
0.42	75.6	0.4995	8.991	0.94	169.2	0.1131	2.036
0.44	79.2	0.4979	8.962	0.96	172.8	0.0778	1.400
0.46	82.8	0.4953	8.915	0.98	176.4	0.0401	0.722
0.48	86.4	0.4917	8.851	1.00	180.0	0.0000	0.000
0.50	90.0	0.4878	8.780				

Figure 2 shows the flexure for measuring longitudinal, i.e., axial, force. The flexure for torque-force measurement was similar but with a 90-degree rotation of the gaged surfaces. The spindle-torque flexure had four thin walls positioned in cruciform. Calibration curves for each flexure were linear and displayed no hysteresis, and each proved to be relatively insensitive to extraneous forces and moments.

Propeller efficiency was not expected to be satisfactory with the use of untwisted, uncambered, rectangular planform blades. Such blades produce high blade-section drag-to-lift ratios because of excessive angle of attack and excessive chord length in the vicinity of the blade tip. It was considered worthwhile to design and test conventional wake-adapted propeller blades for comparison with the rectangular blades to demonstrate a significant advantage in propulsion efficiency. To achieve such a design, use was made of an MIT* design procedure for large-hubbed propeller using lifting-surface design techniques and recognizing the presence of a body of revolution hull form. At the request of this Center, personnel at MIT conducted an efficiency study on the fore and aft propellers of a typical vehicle. The study was restricted to propellers with ratios of hub-to-tip diameter $d/D \approx 0.5$, rpm ranges from 30 to 60, 5-knot full-scale operation, and a 48-foot-long double-ended vehicle of 6-to-1 fineness ratio having a maximum diameter equal to the propeller diameters. The propellers were designed with chordwise load distributions corresponding to the NACA $a = 0.8$ mean line.[3] Predicted radial wake distributions for the fore and aft propellers were also furnished, and although freedom was allowed for the choice of chord-length distribution, it was requested that blade area not be reduced significantly (because of side-force considerations).

The MIT-designed blades for the fore and aft propellers had a maximum chord-length at 40 percent of the span from the root, a thickness-to-chord ratio that ranged from 0.16 at the hub to 0.04 at the tip, and a blade area that was approximately 82 percent of the rectangular blades.

---

*Massachusetts Institute of Technology, Department of Naval Architecture and Marine Engineering.

The camber distributions of the fore and aft propeller designs were different; the greatest differences appeared in the radial pitch distributions that had been adapted to the radial wake distributions at the locations of the fore and aft propellers. Both pitch distributions did, however, exhibit similar trends outside of the severe wake region of the aft propeller ($s/S > 0.2$). This design information was used by the Center to develop a final compromise blade for construction and testing. The compromise design was based on an interpolation between the camber and pitch distributions of the MIT designs for the fore and aft propellers. The choice of the same blade design for both fore and aft propellers appeared justified in view of unavoidable assumptions regarding wake estimates and the fact that the submersible vehicle (and model) had to operate in both astern and ahead motions. The propeller geometry for the final compromise blade design is listed in Table 2.

Figure 3 shows the two propeller-blade configurations tested. The span and blade areas were chosen to ensure significant propeller side-force capability (with the assumption of moderate blade rake.) For simplicity, the two blade shapes will henceforth be designated as rectangular blades and lifting-surface (L-S) blades. The rectangular blades had a span of 8.14 inches and a chord-length of 3.66 inches. These blades were without twist, and their cross section was an uncambered NACA 0016-thickness section.

In accordance with available theoretical and experimental data, the spindle axes were chosen to be 25 percent of the root chord (from the leading edge) for the rectangular blades and 35 percent of the root chord for the lifting-surface blades.

PROCEDURE AND RESULTS

A single rigid strut, located 2 feet from the propeller at the maximum transverse hull section, was used to tow the hull, model both forward and aft to represent the full range of advance coefficient J (based on vehicle speed) from +3.0 to -3.0. Each blade could be adjusted to predetermined values of pitch. Possible pitch-angle settings for the rectangular blades were from +45.0 to -45.0 degrees in 15-degree increments for

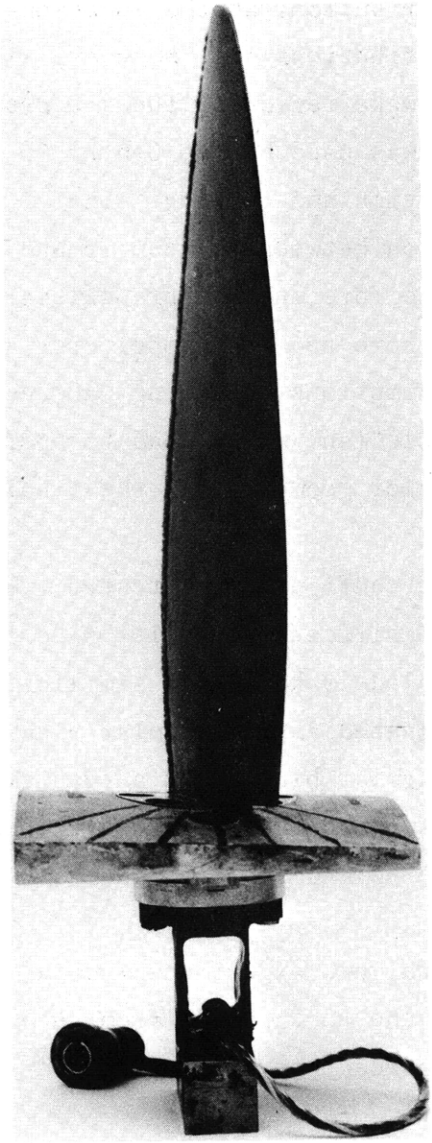

Figure 2 - Blade, Hub Section, and Strain-Gaged Flexure (Axial Force Sensor)

TABLE 2

Geometry of L-S Propeller Blades

s/S	r/R	P/D	c/D	f_M/c	t/c
0.00	0.5063	1.4315	0.0782	0.0238	0.1617
0.05	0.5310	1.4980	0.0858	0.0226	0.1410
0.10	0.5557	1.5607	0.0922	0.0215	0.1258
0.20	0.6051	1.6577	0.1017	0.0195	0.1037
0.30	0.6544	1.7228	0.1068	0.0177	0.0889
0.40	0.7038	1.7578	0.1080	0.0164	0.0782
0.50	0.7532	1.7841	0.1070	0.0155	0.0687
0.60	0.8025	1.8000	0.1016	0.0155	0.0615
0.70	0.8519	1.8065	0.0935	0.0164	0.0506
0.80	0.9013	1.7980	0.0824	0.0192	0.0503
0.90	0.9506	1.7560	0.0658	0.0258	0.0471
0.95	0.9753	1.7189	0.0530	0.0312	0.0481
1.00	1.0000	1.6682	0.000	0.0385	----

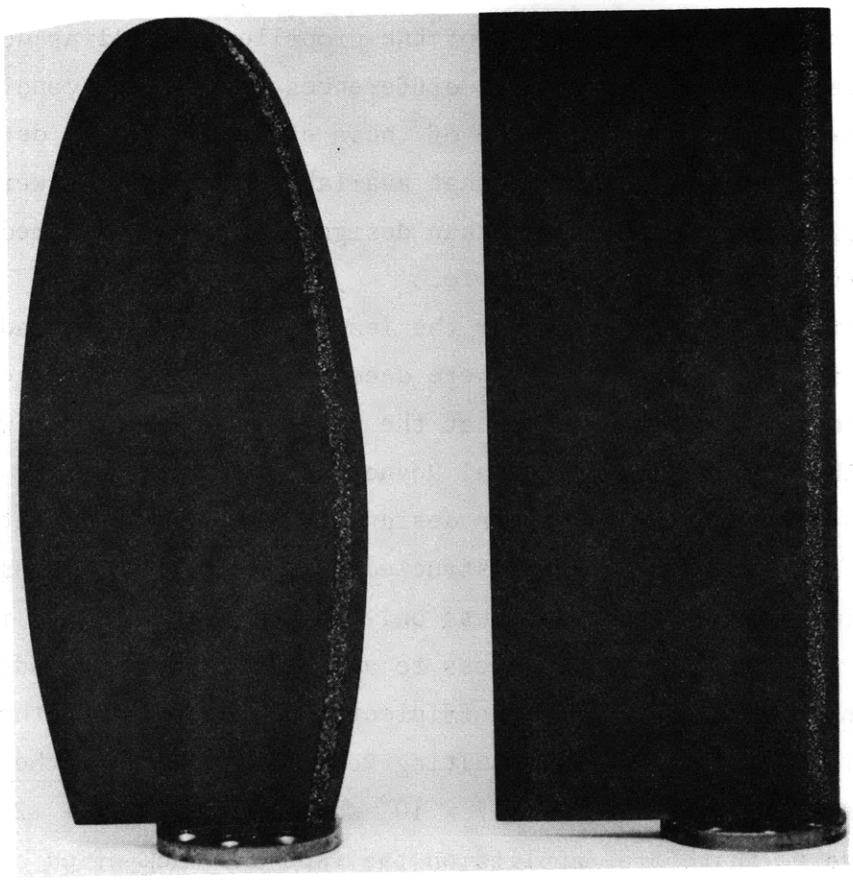

Figure 3 - The Two Blade Shapes Tested

both right-handed and left-handed rotation. The latter capability allowed identical advance conditions to be achieved in runs with the aft portion of the hull and the strut, upstream of the propeller as well as downstream. Since the wakes constituted the only differences in the flow conditions between the two cases, the magnitude of these effects could be determined. The L-S blades were constructed so that available pitch angles were from 15 degrees more to 75 degrees less than design pitch, and intermediate 15-degree pitch settings were possible.

Sand strips were applied near the leading edge of both blade configurations (see Figure 4). These were deemed necessary to trigger turbulent flow when it became apparent that the majority of the tests would be run at less than or near the critical Reynolds numbers. This was because the drive system had originally been designed to drive blades that were considerably smaller than those constructed for these tests. Consequently, the torque limitation of the motor was only 100 inch-pounds, and it was necessary to limit blade torque forces to approximately 2.5 pounds per blade. For the range of advance coefficients $-3.0 \leq J \leq +3.0$, the torque limitation dictated low rpm and resulting Reynolds numbers at the blade midspan r_m were $0.4 \times 10^5 \leq R_n \leq 4.7 \times 10^5$, where $R_n = [c\sqrt{U^2 + (2\pi n r_m)^2}]/\nu$. Sand strips were, therefore, applied on the face and back of each blade, and careful checks were made throughout the tests for possible Reynolds number effects. The sand strips were applied between the 5- and 10-percent chordwide stations with approximately 50 percent of the grains protruding to 0.030 inch from the blade surface. Riegels[4] had indicated that this sand application was more than sufficient to trigger boundary-layer transition.

Data acquisition during testing was accomplished simply by simultaneously monitoring the carriage speed, the model propeller rpm, and the output signals from each of the strain-gaged flexures. All signals were fed into digital voltmeters, and several 10-second averages were recorded. Slight drift was common for the propeller rpm; however, immediate adjustments could be made by continuously monitoring the signal with a 1-second-interval integrating voltmeter. Since a sizeable number of 10-second-average signals were recorded, duplicate data were acquired, and these promised reliable results at each operating condition.

The recorded data indicated that carriage speeds were accurate to approximately 1 percent. Recorded rpm had a possible inherent error of, at most, 1 percent. The possible extent of error in force and moment data depended on the magnitude of the quantities measured. However, a look at the nondimensional force and moment coefficients showed that their accuracy was within the 2- to 3-percent accuracy of the calculated advance coefficient.

The data-acquisition procedure described previously permits the collection of only steady-state data. No attempts were, or could be, made to obtain dynamic forces and moments mainly because of the difficulty in determining instantaneous propeller rpm.

The following assumptions were made in the data analysis.

1. Since only axial force, torque force, and spindle-moment measurements on individual blades were made, blade torque had to be estimated. This necessitated choosing a radial location on the blade where the resultant torque force was estimated to be acting. Lifting-line-theory calculation showed that the effective radius of torque force for the blade geometries tested was, at most, 80 percent of the blade span from the hub. This value probably produced conservative estimates in many cases, but it was used throughout the calculations of blade torque.

2. Although performance estimates for cyclic pitch are presented herein, no cyclic-pitch tests were run. In each test, all six propeller blades were pitched identically to one of the incremental pitch angles. Since cyclic-pitch operation is a completely dynamic condition and since no dynamic data were derived from the tests, the estimates given herein are from steady-state tests.

3. The test data were extrapolated to predict propeller side-force capability in the presence of cyclic-pitch operation and blade rate. Although the test apparatus employed blades without rake, it is reasonable to assume that they represented geometrically similar blades that might be raked relative to some transverse hull plane but might still remain normal to the local hull slope at their point of attachment. However, it is also reasonable that raked blades of identical span would suffer a reduction in loading due to the reduction of the effective radius from the propeller axis and the consequent reduction in local tangential

velocity. By restricting the evaluations to the case of zero vehicle advance, however, it was possible to make a valid prediction of side force by assuming that an increase in rpm will counter the reduction in local velocity due to blade rake. Blade lift and, hence, the angle of attack α can then be considered unchanged. Nondimensional force and moment coefficients, however, will show the effects of blade rake due to their inverse proportionality to (n^2).

To eliminate the presence of hub-section effects of blade force and moment measurements, a complete set of no-load tests was run in which the full ranges of advance coefficients and rpm were covered without the blades in place. Flanges were installed flush with the hub sections at the blade-mounting positions to avoid possible drag sources. From the no-load test runs, axial forces, torque forces, and moments on the hub section were determined as functions of vehicular speed and rpm, and the results were available for subtraction from the total measured quantities in tests made subsequently with blades in place.

No-load values have been removed from the actual measurements of the test data presented here, and the plots show only blade characteristics. The sign conventions are consistent throughout the data and are as follows:

1. Positive torque is that moment opposing the rotation of the hub.
2. Positive thrust is the force generated by the blade in the direction of the hull bow.
3. The positive spindle moment is the right-hand or counterclockwise moment on the hub section as viewed from outside the model.

Figure 4 shows the drag forces measured for the rectangular blades at zero pitch and zero advance for blades with a single sand strip on the blade back, with sand strips on the blade face and back, and with no sand strips. Similar tests were run at a 30-degree pitch angle in the hope that the sand-strip drag could be systematically determined and subtracted from all blade side-force results. When analyzing the results, however, it appeared that the drag subtraction was impossible. Tests of the rectangular blades at zero pitch and at other than zero advance showed that for small angles of attack, the sand-strip drags were higher than at zero angle of attack and that at sizeable angles of attack, the drag

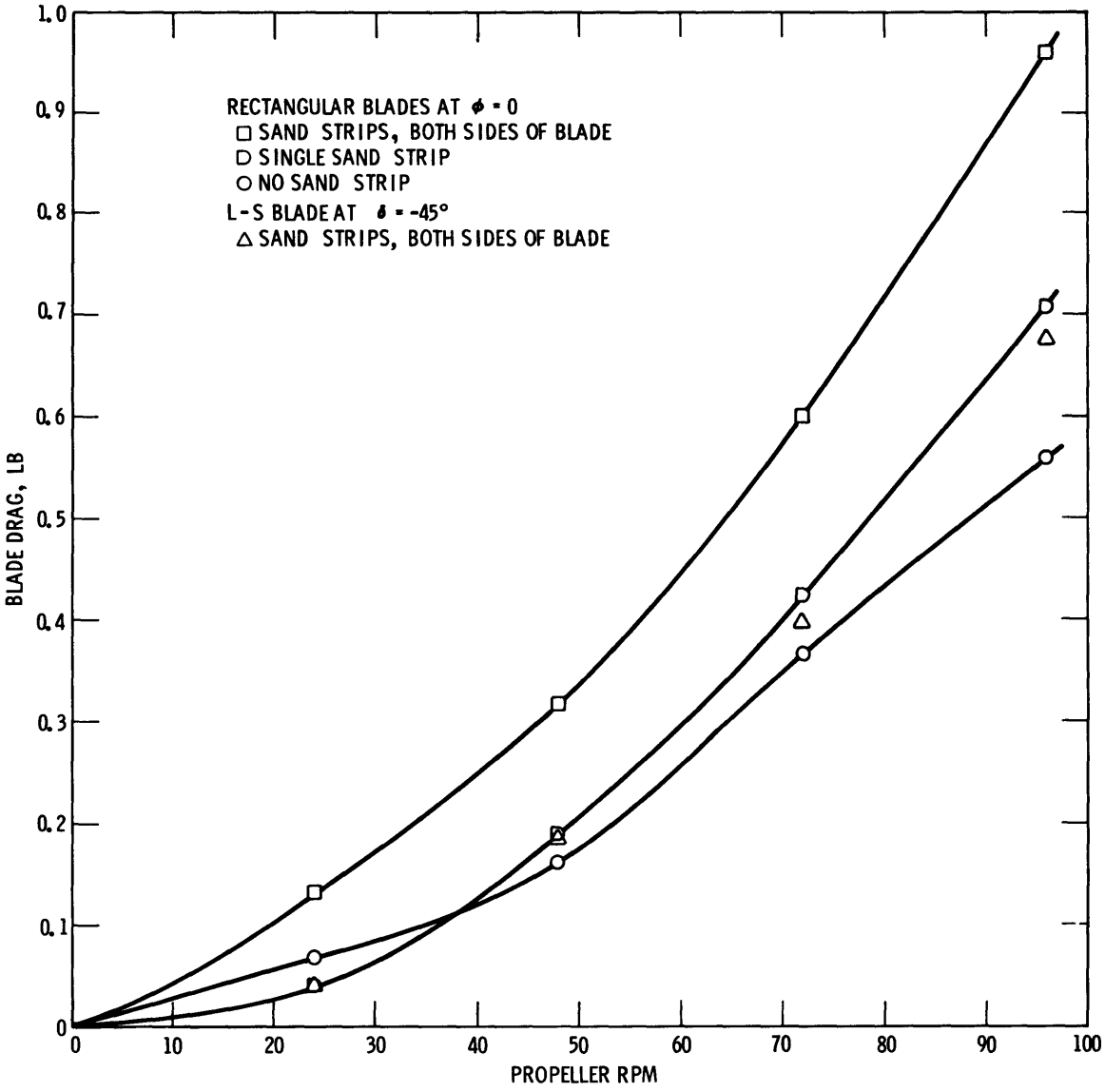

Figure 4 - Blade Drags at Zero Advance Coefficient Showing Effects of Sand-Strip Applications

effects were less. Consequently, no sand-strip drag was removed from the data, and all data that follow are from tests with blades having sand strips on both the faces and the backs.

Figure 4 also shows the blade drag for the lifting-surface blade at zero advance and at δ = -45 degrees (45 degrees below design pitch). Although the L-S blade has a varying radial pitch and the rectangular blade does not, its drag at zero advance is considerably less than that of the rectangular blade. This phenomenon is due in part to the high-drag characteristics of the rectangular blade tip.

Figures 5 and 6 show the nondimensional thrust and torque coefficients for the rectangular and lifting-surface blades of propellers, respectively, as functions of advance coefficient and blade pitch. These results were for right-handed hub rotation. A positive advance coefficient J indicates ahead motion of the model, i.e., U > 0, and a negative advance coefficient indicates astern motion. The advance conditions were duplicated for left-handed hub rotation and with the hull model moving astern; although thrust results were slightly higher and torque results were nearly identical, the overall differences were insignificant and were not worthy of presentation. Testing in both right-handed and left-handed regimes did furnish substantial aid in cross checking results.

Figure 7 shows the resulting efficiency curves for the rectangular-bladed propeller and for the L-S bladed propeller. As expected, the more sophisticated blade shape is considerably more efficient. Also, if one considers that at an advance coefficient near J = 1.8, each radial section of the L-S blade is operating near a zero angle of attack and that a subtraction of sand-strip drag is feasible, then calculations show the efficiency peaking at greater than 80 percent. This is not indicated on the efficiency plot, however, since it is not known what the effects might be for the other portions of the curve or for any segments of the curves representing the rectangular blade efficiencies.

Figures 8, 9a, and 9b are plots of nondimensional spindle torques for individual blades of the rectangular and lifting-surface bladed propellers. As mentioned before, the spindle axis for rectangular blades was located at 25 percent of the chord length from the blade leading edge. For the lifting surface blades, the location was set at 35 percent of the chord length.

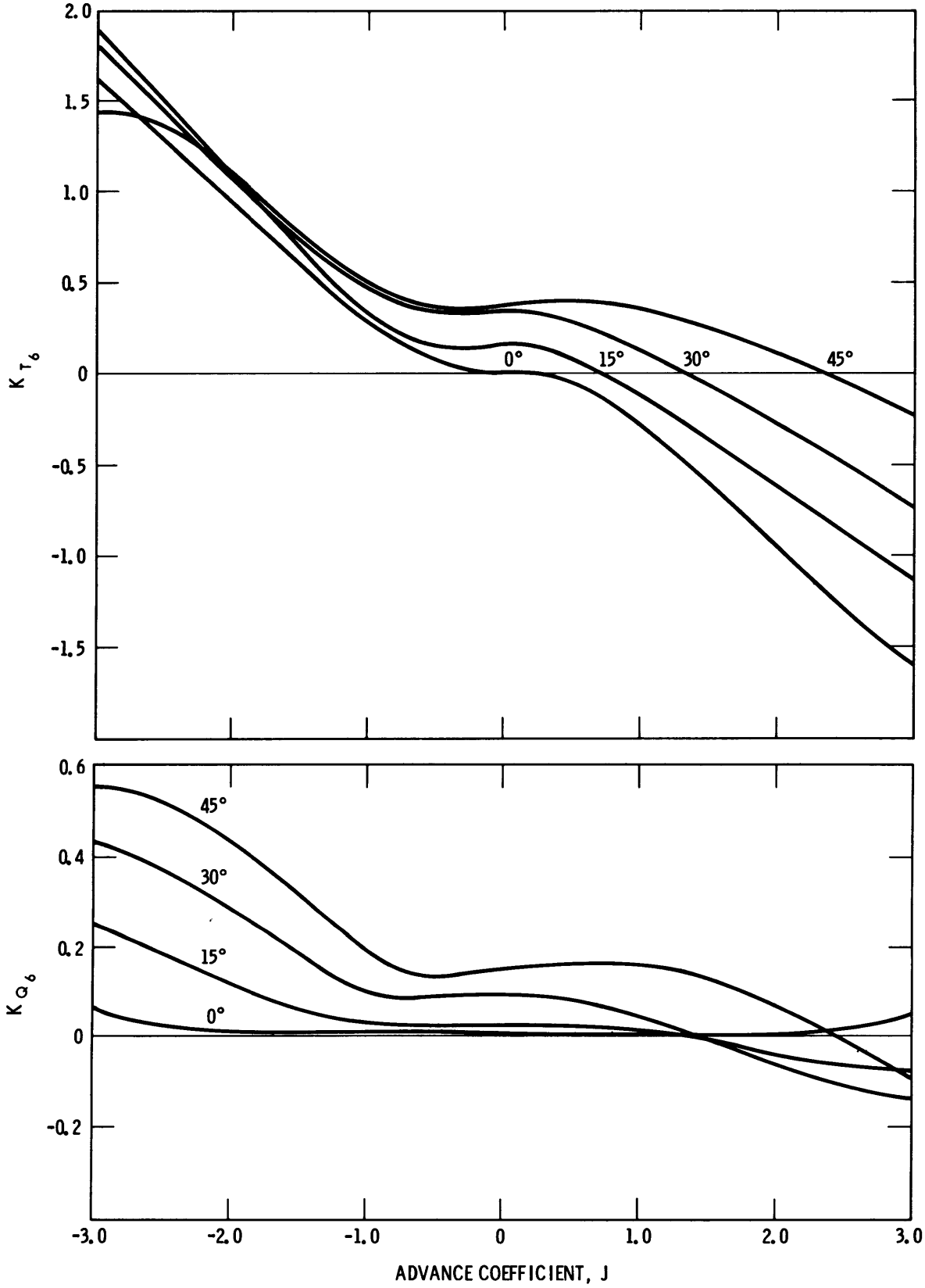

Figure 5 - Thrust- and Torque-Coefficient Curves for Rectangular Blades at ϕ = 0, 15, 30, and 45 Degrees

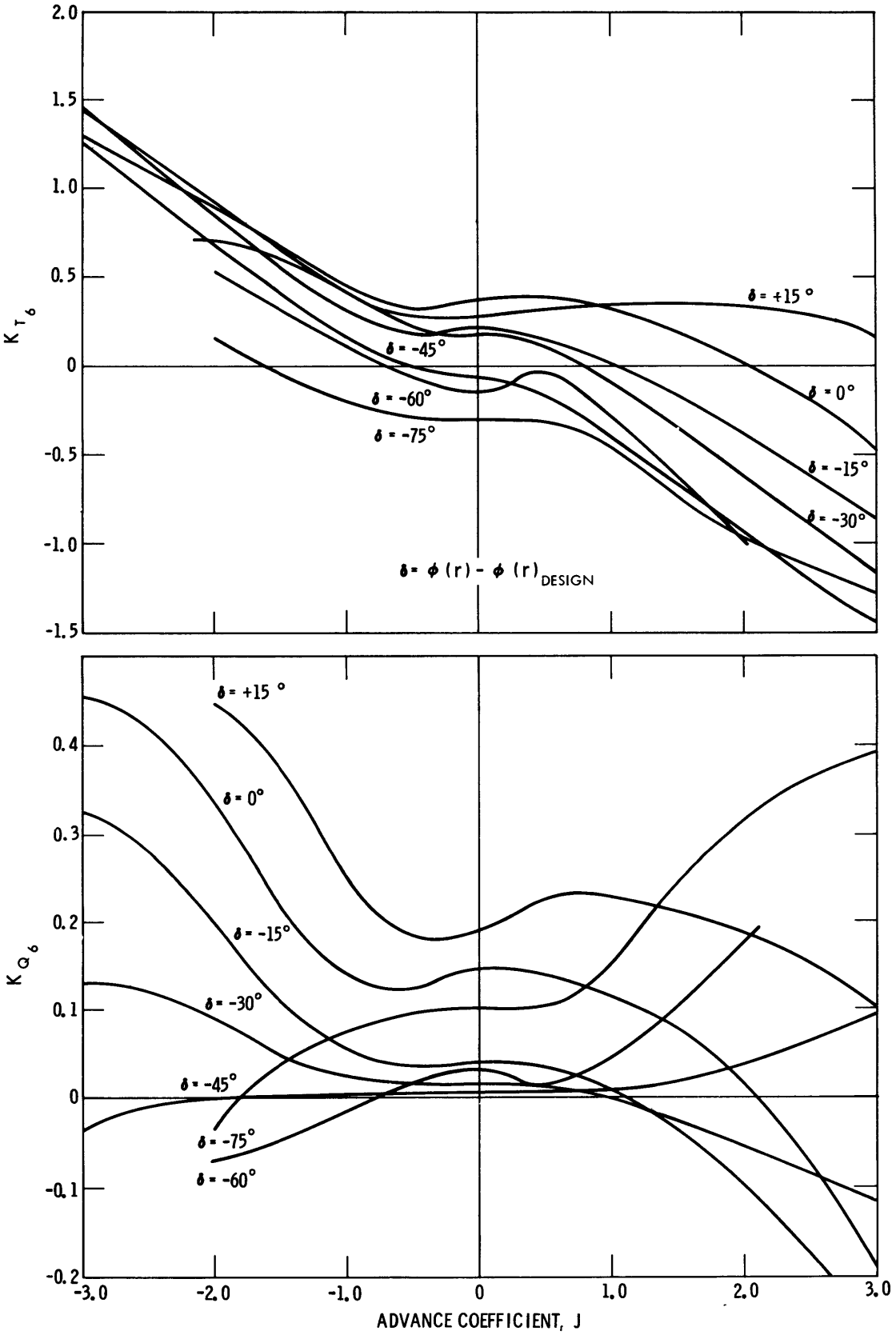

Figure 6 - Thrust- and Torque-Coefficient Curves for L-S Blades at δ = +15 to δ = -75 Degrees

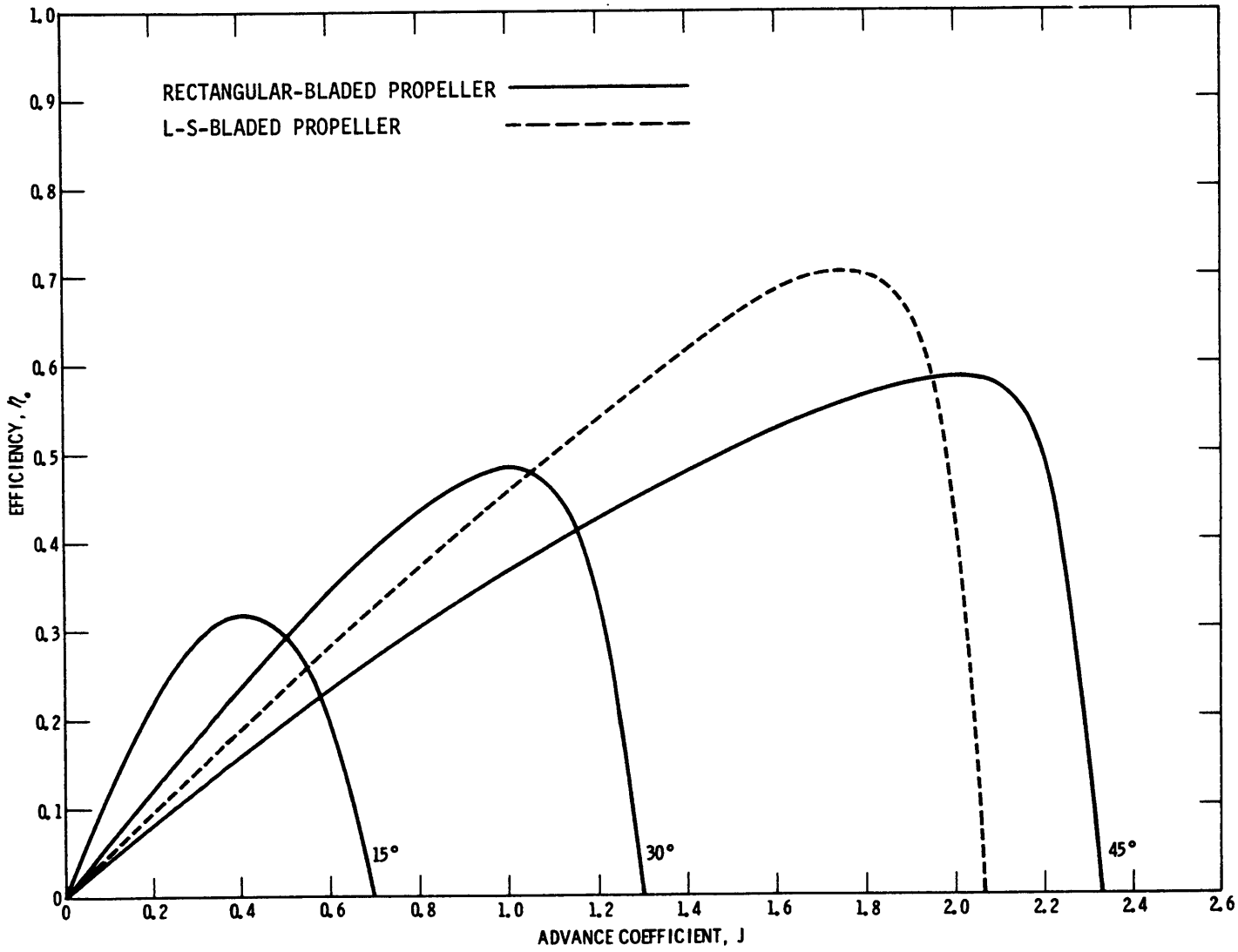

Figure 7 - Efficiency Curves for Rectangular Blades at ϕ = 15, 30, and 45 Degrees and for L-S Blades at Design Pitch, δ = 0

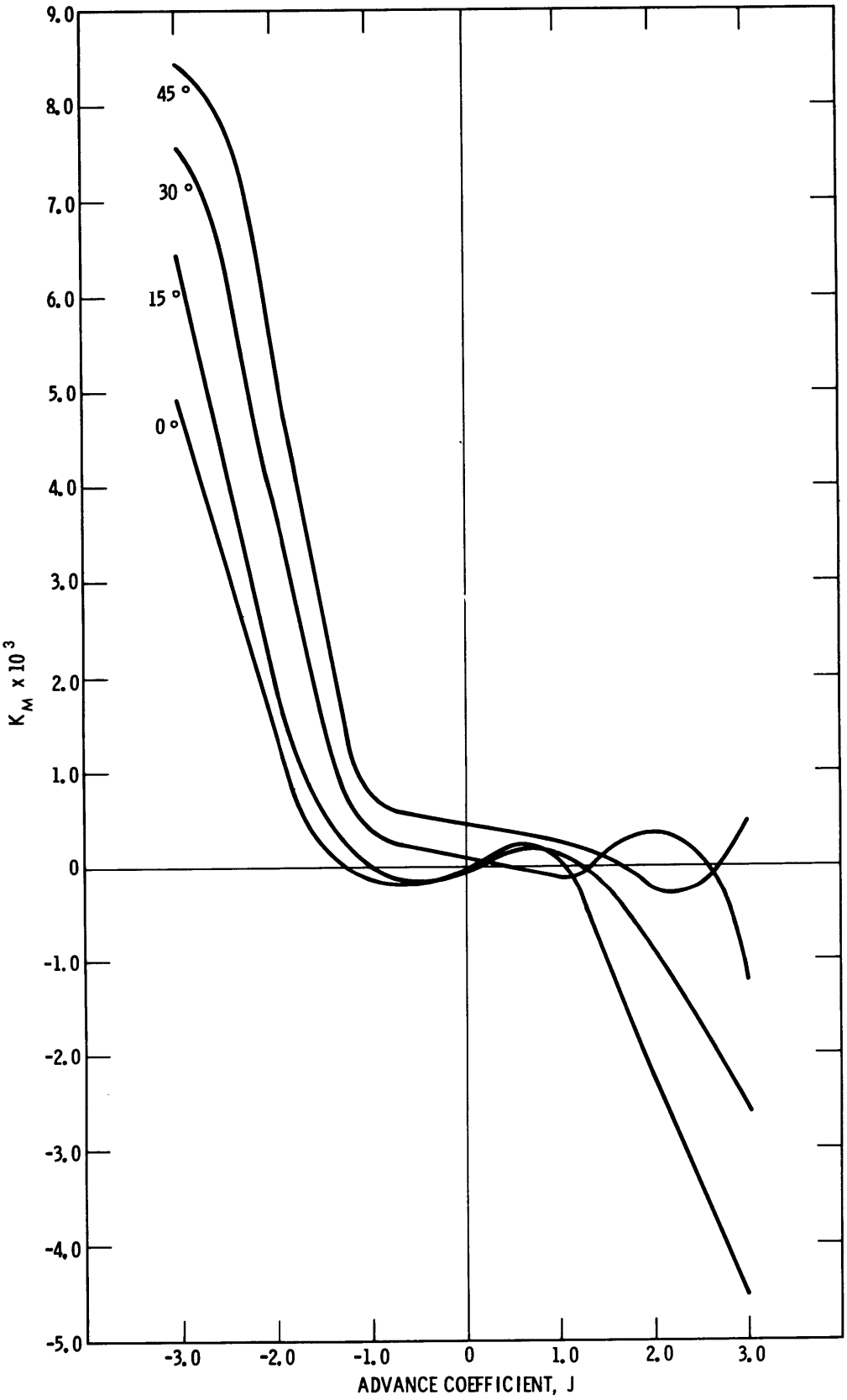

Figure 8 - Single-Blade Spindle Torque Coefficients for Rectangular Blades

Figure 9 - Single-Blade Spindle Torque Coefficients for L-S Blades

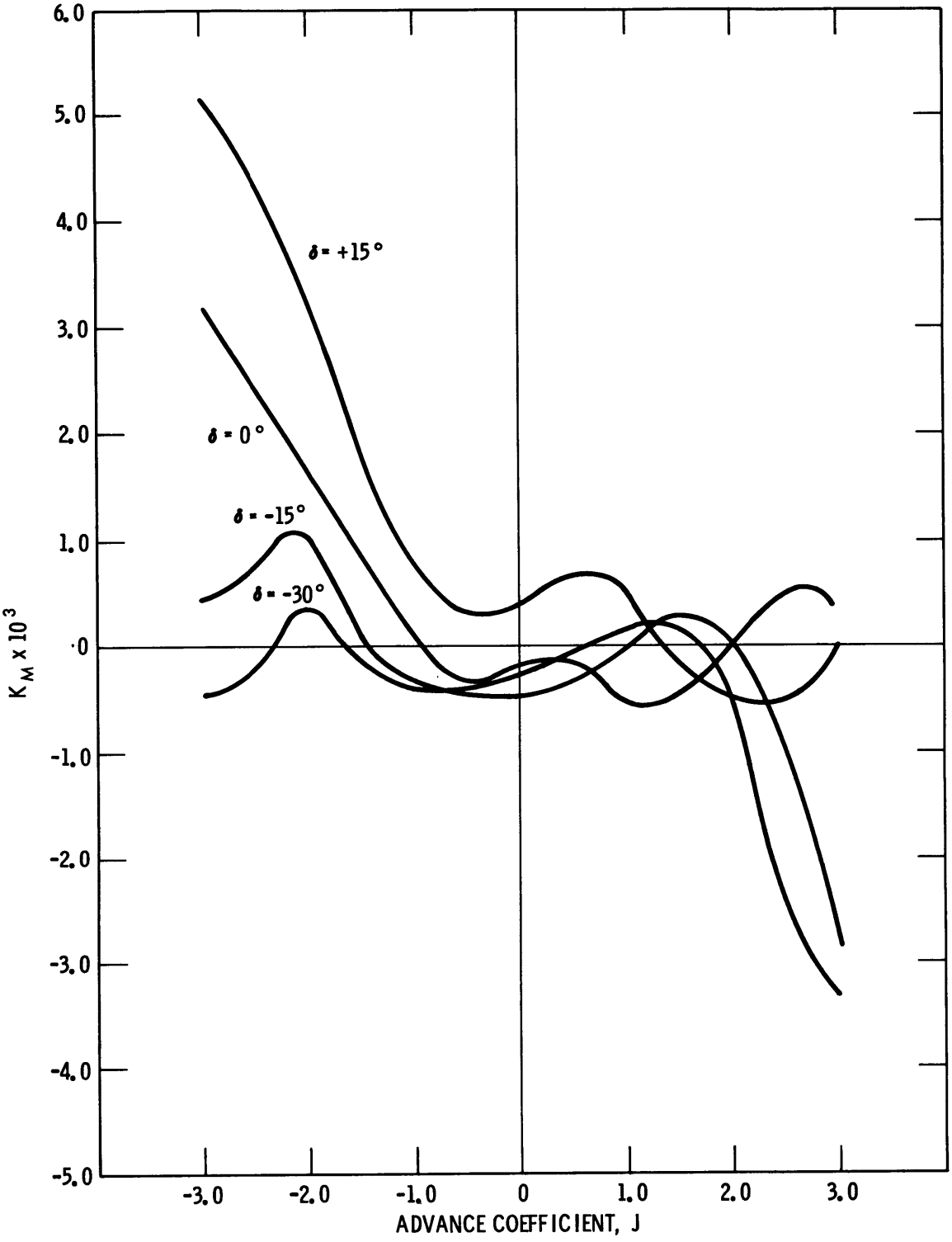

Figure 9a - δ = +15, 0, -15, and -30 Degrees

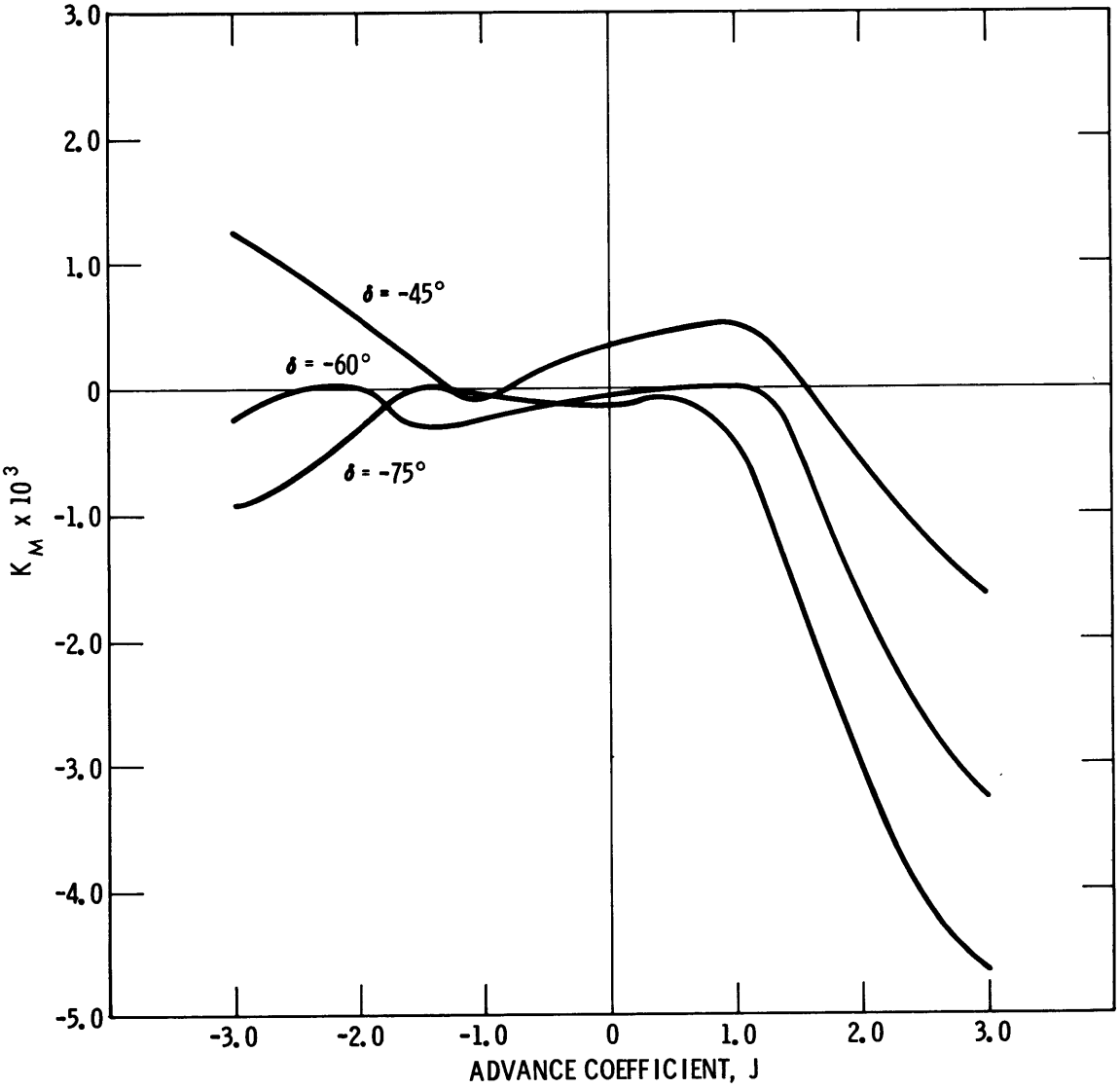

Figure 9b - δ = -45, -60, and -75 Degrees

Figure 10 shows the single-blade thrust and torque coefficients for both blade configurations at zero advance coefficient and for the full range of pitches covered in the tests. As expected, the thrust curve for the rectangular blade was nearly linear up to approximate stall at 30 degrees. The thrust-coefficient curve for the L-S blade was not expected to be linear; however, the degree of irregularity apparent in that curve was not anticipated. Numerous checks on repeatability and rpm effects were performed during testing to confirm the data, and no questionable measurements or Reynolds number effects were found to contribute to the irregularity of the curve. Similar but less pronounced irregularities have been reported for the thrust-coefficient curves of controllable pitch propellers operating at zero advance;[5] the only explanation for the trend seems to be the varying effectiveness of hub and midspan blade sections of cambered and twisted blades at off-design pitch and advance conditions. Should this be true, then the greater effectiveness of hub sections of large-hubbed propeller blades could add to the irregularity present in the K_T curve of Figure 10.

The quantities shown in Figure 11 were derived from the curves of Figure 10. Using the assumption that blade rake reduces the effective blade loading, i.e., both the thrust and torque components, the effects on side-force capability of blade rake and cyclic pitch were calculated for the rectangular-bladed propeller. Cyclic-pitch amplitude is defined as the half amplitude of the pitch variation, and the circumferential pitch variation is assumed to be sinusoidal.

Figure 12 shows the predicted ratios of side force to power and the propeller rpm necessary for a 35-degree raked, six-bladed full-scale propeller to produce 300 pounds of side force. Curves for both rectangular-bladed and L-S-bladed propellers are shown. The superimposed symbols on the curves of the L-S propeller show one condition in which aft and forward propellers would cancel each other in axial force generation. A rectangular-bladed propeller is expected to produce a net axial thrust of zero at any sinusoidal cyclic pitch that is symmetric about $\phi = 0$ degrees, but such is not the case for propellers with more sophisticated blade geometries. The three conditions that must be satisfied in pure hover

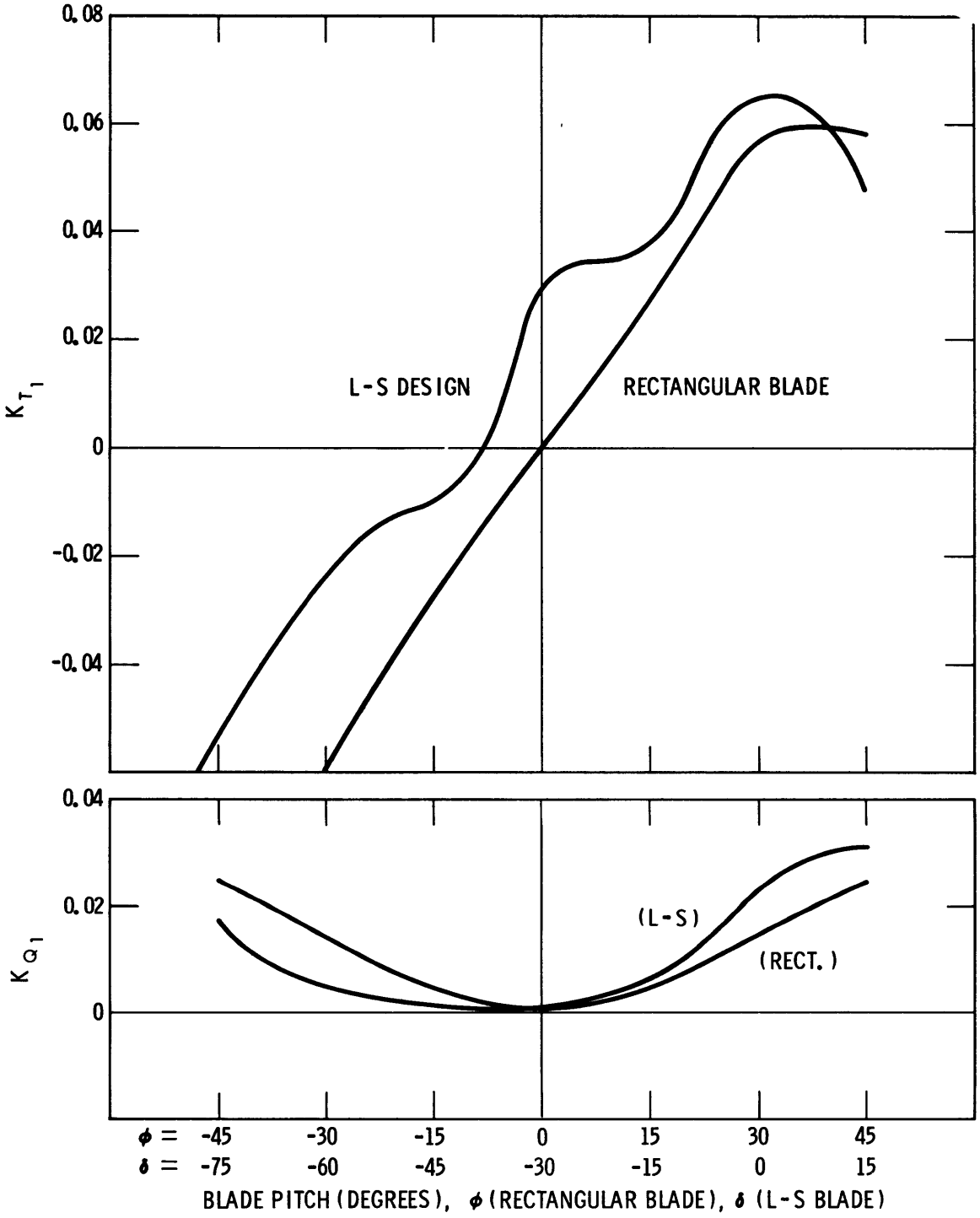

Figure 10 - Single-Blade Thrust and Torque Coefficients for Rectangular and L-S Blades at Zero Advance for a Range of Blade Pitches

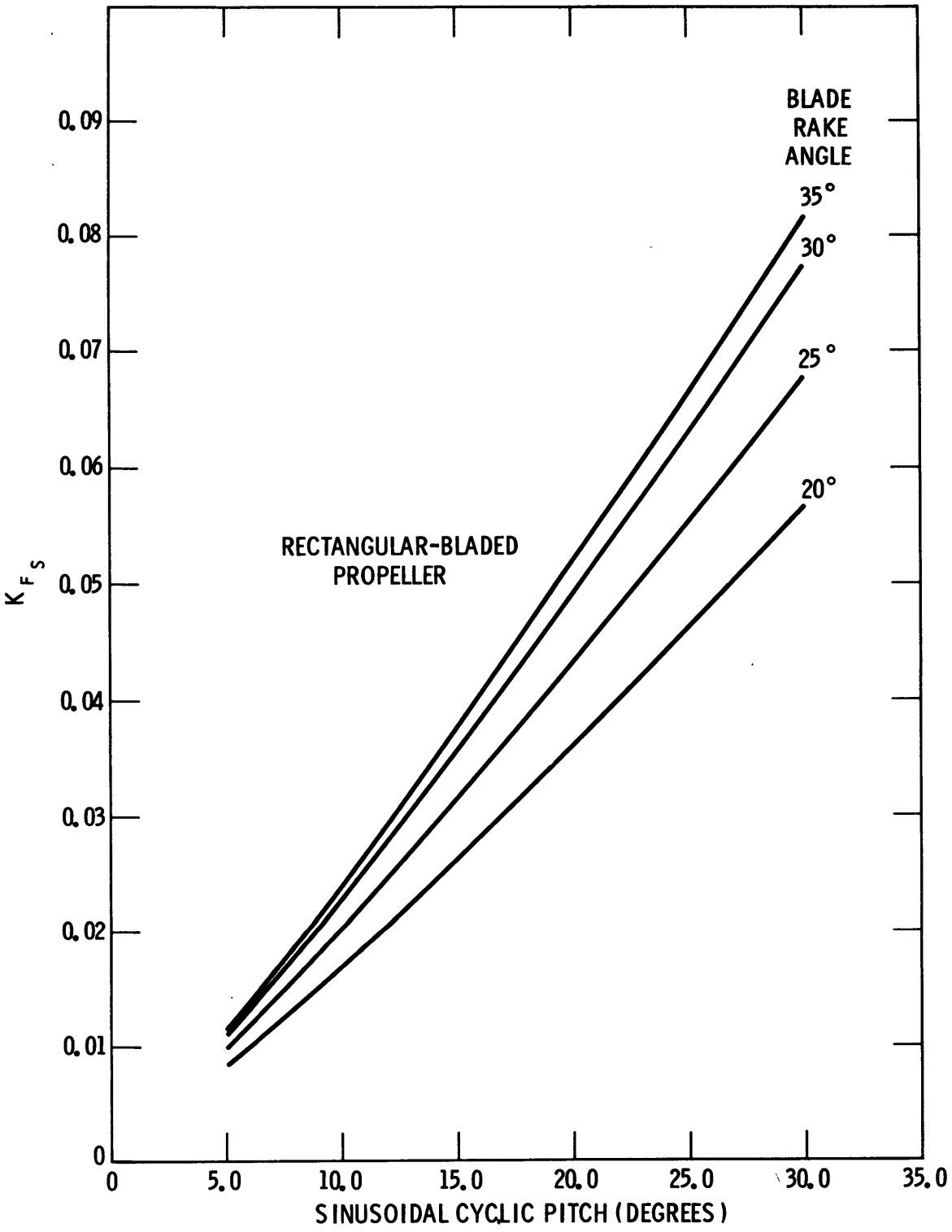

Figure 11 - Side-Force Coefficients for the Rectangular-Bladed Propeller as a Function of Blade Rake and Cyclic Pitch at Zero Advance

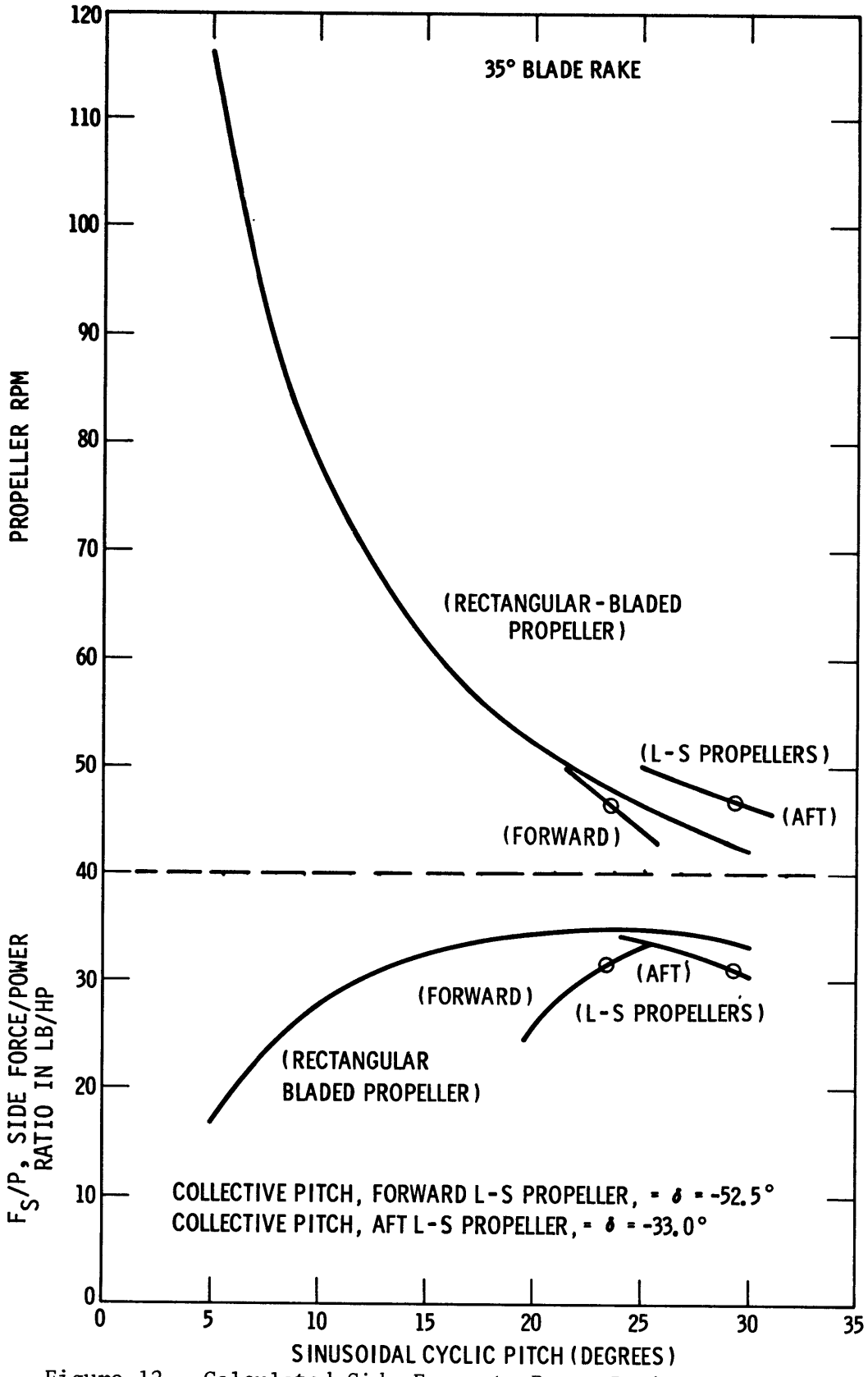

Figure 12 - Calculated Side Force-to-Power Ratios, Evaluated at 300 Pounds of Side Force per Propeller

between the aft and forward propellers of a vehicle are torque balance (within reason), identical side-force production, and a collective net axial thrust of zero. It appears from the calculations that such an operating condition is feasible with complicated blade geometries but control will be somewhat limited because of the basic asymmetry of the propellers.

DISCUSSION

In addition to furnishing the data for blade forces and moments discussed in the project objectives, the test results yielded other information worthy of discussion. Note in Figure 5 that the thrust-coefficient curves for the rectangular-bladed propellers are closely spaced for advance coefficients less than $J = -1.0$. Had plots been shown for the results at negative pitches over the full advance-coefficient range, the same trends would have been apparent in the negatively pitched blade-thrust curves at advance coefficients greater than $J = 1.0$. The importance of these data characteristics is that they occur in the probable advance ranges of full-reverse or full-ahead emergency maneuvers. For instance, an inspection of the 0- and the 45-degree pitch curves at an advance coefficient of $J = -2.0$ reveals that similar production of positive thrust could be expected at identical rpm, and yet the torque of the zero-pitched blade is far less. This indicates that the appropriate blade pitch for minimum power absorption of rectangular-bladed propellers during full-reverse (or full-ahead) maneuvers is zero pitch rather than a sizeable negative (or positive) pitch. The same statements hold true for the more complicated L-S-blade configuration except that one must apply nearly zero average radial pitch settings because of the presence of spanwise blade twist.

Since the tests were run at low rpm and at near-critical Reynolds numbers, special care was taken to check for possible laminar-flow effects. The checks were performed by repeating certain tests at identical advance coefficients but with different vehicular speeds and rpm. It was found that the nondimensional thrust- and torque-coefficient curves at a particular advance coefficient would remain flat until some low rpm value was reached; then a definite increase or decrease in the curve would occur.

The transition point for both thrust and torque coefficients occurred at approximately the same rpm. However, the same tests showed that spindle torque was far more sensitive to rpm than were thrust and torque. A probable explanation lay in discussions of the resultant pressure distributions on the blade surfaces. It is conceivable that slight rpm changes might shift sectional pressure distributions and although the local nondimensional thrust and torque were unaffected, the differences in resultant pressure distributions on either side of the blade-spindle axis could be significant.

The test results may also be of value in another area of spindle-torque prediction. As mentioned before, although the data were all taken in the steady-state condition, it is possible to make certain estimates of power requirements of dynamic spindle torque in cyclic pitch. Since it is the inability to determine an instantaneous blade angle of attack during cyclic pitch that leads to the inadequacy of using steady-state results to predict dynamic quantities, it follows that highly conservative estimates of the attack angles will at least lead to rough but safe estimates. An example of such a calculation would be an estimate of the power required in blade-turning effort to produce cyclic pitch at zero advance. If one chooses conservative spindle-torque coefficients for a single blade, then the instantaneous power required for one blade can be calculated as follows:

$$P_1 = M_1 \frac{d\alpha}{dt}$$

where M_1 is the dimensional spindle torque and $d\alpha/dt$ is the rate of change of angle of attack during cyclic pitch, i.e., for a sinusoidal cyclic pitch, α could be approximated as

$$\alpha = A \sin 2\pi nt$$

where A is the cyclic pitch amplitude in radians,

n is the propeller rpm, and

t is time.

CONCLUSIONS

From the results of tests and analyses described in this report, the following conclusions and recommendations are made for large-hubbed propellers and their applications.

1. Design criteria that call for sizeable propeller side-force capability and good propulsive efficiency in the ahead operational mode contain conflicting requirements. The need for side-force generation will lead to blade areas and blade spans that are greater than would be recommended from the standpoint of efficient ahead propulsion.

2. Rectangular or foil-type blades without spanwise twist or section camber are much better for side-force generation and maneuvering since the geometric symmetry of the blades and, therefore, the symmetry of the propeller during pure cyclic-pitch operation lead to a cancellation of axial thrust generated at the propeller.

Propellers with plane rectangular blades tend to be inefficient during any cruise condition because of the higher blade-section angles of attack that result from the large differences between the blade-section pitch and the hydrodynamic inflow over portions of the blade. Also, for low thrust requirements, blade-section angles of attack may vary from negative to positive from hub to tip, respectively, and the operation is therefore far from the peak efficiency possible with the L-S-type blade configuration.

3. Large-hubbed propellers can be highly efficient when equipped with blades that have been designed for a particular operating advance coefficient and that have diminishing chord lengths and blade thickness toward the tip. However, an inspection of these propellers in maneuvering modes and pure side-force generation reveals that they will have limited controllability because of the geometric asymmetry of the propellers and the resultant axial thrust components that are generated.

4. When selecting blade geometries for large-hubbed propellers, the importance of various facets of the mission of the vehicle should be carefully weighed. If most of a projected mission consists of vehicular operation in a cruise mode, then, to preserve power, an efficient blade

shape should be employed. If maneuverability is the main consideration, then controllability is important, and a simple blade shape should be employed.

5. In view of the previous conclusions, it is recommended that a hybrid blade design be investigated. A blade shape with diminishing section thickness toward the tip and reduced chord lengths at the tip but without section cambers or spanwise twist should be considered in a trade-off study between maneuverability and ahead propulsion.

6. The effects of increased blade rake should also be investigated. Increased blade rake offers the possibility of improved side-force capability without increased blade area or blade span.

ACKNOWLEDGMENT

The author wishes to thank Mr. August J. Fontana for his assistance in preparing the test apparatus and testing the models.

REFERENCES

1. Haselton, F.R., Jr., "Submarine Hydrodynamic Control Systems," U.S. Patent 3, 101, 066 (20 Aug 1963).

2. Lindenmuth, W.T. and Barr, R.A., "Propulsion and Static Stability Tests of a Tandem Cyclic Pitch Propeller for a Deep Sea Rescue Submarine," Hydronautics, Inc. Technical Report 601-1 (1 Feb 1968).

3. Abbot, I.H. and Doenhoff, A.E.V., "Theory of Wing Sections," Dover Publications (1959).

4. Riegels, F.W., "Aerofoil Sections," (translated by D.G. Randall). Butterworth & Company, Ltd., London (1961).

5. Hansen, E.O., "Thrust and Blade Spindle Torque Measurements of Five Controllable-Pitch Propeller Designs for MSO-421," NSRDC Report 2325 (Apr 1967).

INITIAL DISTRIBUTION

Copies	
5	NAVSHIPS 3 SHIPS 2052 1 SHIPS 033 1 SHIPS 031
6	NAVSEC 1 SEC 6100 2 SEC 6110 1 SEC 6144 2 SEC 6148
1	NAVORDSYSCOM (Ord 05411)
2	NAVAIRSYSCOM 1 Air 604 1 Air 302
2	CHONR 1 Fluid Dyn (Code 438) 1 Sys and Res Gp (Code 492)
1	CDR, NUWC
1	CDR, NWC
1	CDR, USNOL
1	DIR, USNRL
1	ONR, SAN FRAN
1	CO, ONR, BSN
1	CO, ONR, Pasadena
1	CO, ONR, Chicago
1	ONR(L)
1	NAVSHIPYD PTSMH
1	NAVSHIPYD BSN
1	NAVSHIPYD BREM
1	NAVSHIPYD PHILA
1	NAVSHIPYD CHASN
1	NAVSHIPYD LBEACH
1	CDR, NWL Attn Computation & Exterior Ballistics Lab
1	CO, USNROTC & NAVADMINUMIT
1	SUPT, USNA
1	USNASL, Attn Lib

Copies	
1	CO, USNAVUWRES, Attn Lib
1	CDR, NELC, Attn Lib
1	CO & DIR, USNAVCIVENGRLAB
1	NNS&DD, Eng Technical Dept
6	DSSP, SP-11-223
1	USNAVPGSCOL, Monterey
20	DDC
1	NASA, Attn Dr. W.L. Haberman (Code MTY)
2	ADMIN, MARAD 1 Attn Ship Div 1 Attn Coordinator of Research
1	CO, MSTS
1	BUSTAND, Attn Lib
1	SUPT, USMA
1	Commandant, USCOGARD Attn: Ship Construction Comm
1	Commander, U.S. Army Transportation Res & Dev, Fort Eustis, Va, Attn Marine Transportation Div
1	Air Force Office of Sci Res, Washington, Attn Mechanics Div
1	W-PAFB, Dayton Attn Wright Air Dev Div, Aircraft Lab
2	Langley Res Center, Langley Station, Hampton, Va 1 Attn Mr. I.E. Garrick 1 Attn Mr. D.J. Marten
1	DIR, Nat'l Sci Foundation, Washington, Attn Eng Sci Div
1	Chief of Res & Dev, Office of Chief of Staff, Dept of the Army, the Pentagon
1	DIR, WHOI
1	NASA, College Park Attn Sci & Tech Info, Acquisitions Br

Copies	
1	Commander Gen, Army Eng Res & Dev Lab, Fort Belvoir, Va Attn Tech Documents Center
1	DIR, ORL, Penn State
2	MIT 1 Head, Dept NAME 1 Prof J.E. Karman
3	CIT 1 Attn Prof Acosta 1 Attn Prof Plesset 1 Attn Prof Wu
1	DIR, St. Anthony Falls Hydra Lab, Univ of Minn, Minneapolis
1	Univ of Notre Dame, Dept of Mech Eng, South Bend
1	DIR, Inst of Hydraulic Res, Univ of Iowa, Iowa City
1	Univ of Michigan, Dept NAME, Ann Arbor
1	Univ of Calif, Berkeley 1 Attn Head, Dept NAVARCH
2	State Univ of Colorado, Fort Collins, Colorado 1 Attn Dr. M.L. Albertson 1 Attn Prof J.E. Germak
1	Cornell Univ, Graduate School of Aeronautical Eng, Ithaca
2	JHU, Baltimore 1 Attn Dept of Mechanics 1 Attn Inst of Cooperative Res
2	State Univ of New York, Maritime College, Bronx, N.Y. 1 Attn Engineering Dept 1 Attn Inst of Math Sciences
1	Stanford Univ, Stanford, Calif Attn Dept of Civil Eng
1	Univ of Illinois, Dept of Theoretical & Applied Mech, Urbana
1	Cornell Aeronautical Lab, Buffalo
2	Davidson Lab, SIT, Hoboken 1 Attn Director 1 Attn Dr. Tsakonas

Copies	
1	Rensselaer Polytechnic Inst, Dept of Math, Troy, N.Y.
1	Puget Sound Bridge & Drydock Co, Seattle
1	Douglas Aircraft Co, General Applied Sci Lab, Westbury, L.I., N.Y.
1	ITEK Corp, Vidya Div, Palo Alto
1	TRG Inc, Melville, N.Y.
1	Therm Inc.
1	Lockheed Missiles & Space, Sunnyvale Attn Dept 5701
1	Electric Boat Co, General Dynamics Corp, Groton
1	Robert Taggart Inc, Fairfax, Va
1	Oceanics
1	Gibbs & Cox
1	George G. Sharp, Inc.
1	Grumman Aircraft Corp., Bethpage
1	Hydronautics, Inc.
1	Martin Co, Baltimore
1	Boeing Aircraft, AMS Div, Seattle
1	United Aircraft, Hamilton Standard Div, Windsor Locks, Conn
1	AVCO, Lycoming Div, Washington
1	Baker Mfg, Evansville
2	Sperry Systems Mgmt Div, Great Neck 1 Attn Mr. R.S. Brannin
2	General Dynamics - Convair, San Diego 1 Attn Dr. B.R. Parkin 1 Attn Chief of ASW/ Marine Sci

Copies	
1	Curtiss-Wright Corp, Woodridge, N.J.
1	FMC
1	President, Gen Tech Services Inc, Cleveland
1	Dr. S.F. Hoerner, 148 Busteed Drive, Midland Park, N.J.
1	RCA, Burlington, Mass Attn Hydrofoil Projects
1	U.S. Rubber Co, Res & Dev Dept, Wayne, N.J.
1	North American Aviation Inc, Oceans Systems Div, Downey, Calif
1	Aerojet-General Corp, Azusa
1	SNAME
1	ASNE, Washington
1	ASME, Res Comm in Information, New York
1	Inst of Aerospace Sciences, New York Attn Lib
1	Westinghouse Elect Corp Annapolis

UNCLASSIFIED

Security Classification

DOCUMENT CONTROL DATA - R & D

(Security classification of title, body of abstract and indexing annotation must be entered when the overall report is classified)

1 ORIGINATING ACTIVITY (Corporate author)	2a. REPORT SECURITY CLASSIFICATION
Naval Ship Research & Development Center Washington, D.C. 20007	Unclassified
	2b. GROUP

3 REPORT TITLE

MEASUREMENT OF FORCES AND SPINDLE MOMENTS ON INDIVIDUAL BLADES OF A LARGE-HUBBED PROPELLER

4 DESCRIPTIVE NOTES *(Type of report and inclusive dates)*

5 AUTHOR(S) *(First name, middle initial, last name)*

Stephen B. Denny

6 REPORT DATE	7a. TOTAL NO. OF PAGES	7b. NO. OF REFS
December 1969	37	5

8a. CONTRACT OR GRANT NO.	9a. ORIGINATOR'S REPORT NUMBER(S)
b. PROJECT NO. SS-4636-0000	3252
c. Task 12320	9b. OTHER REPORT NO(S) *(Any other numbers that may be assigned this report)* AD 700 909
d.	

10. DISTRIBUTION STATEMENT

This document has been approved for public release and sale; its distribution is unlimited.

11. SUPPLEMENTARY NOTES	12 SPONSORING MILITARY ACTIVITY

13. ABSTRACT

Axial forces, torque forces, and spindle moments were measured on the individual blades of a six-bladed large-hubbed propeller ($d/D \simeq 0.5$). Two different propeller-blade configurations were tested, and the hydrodynamic characteristics of each were determined over wide ranges of blade pitch and advance conditions. The experimental results indicated the peak forces and moments on propeller blades during emergency operating conditions as well as blade loads and propeller efficiencies during normal cruise operation. Also, by assuming a given blade rake relative to the propeller rotation plane and by vector resolution of the blade forces determined at zero advance for various pitches, it was possible to calculate the extent of propeller side-force capability during cyclic pitch operation.

The test results show that a mission requirement for large-hubbed cyclic-pitch propellers which calls for sizeable side-force capability for maneuvering will dictate the use of large blades that are not efficient in vehicle cruise modes. Recommendations are made for further investigations of blade-configuration and blade-rake effects on both propeller side-force capability and ahead propulsion.

14 KEY WORDS	LINK A		LINK B		LINK C	
	ROLE	WT	ROLE	WT	ROLE	WT
Controllable-Pitch Propellers						
Cyclic-Pitch Propellers						
Large-Hub Propellers						
Submarine Propulsion						
Propeller Blade Spindle Torque						